Journal of Environmental Radioactivity 166 (2017) 296–308

Contents lists available at ScienceDirect

Journal of Environmental Radioactivity

journal homepage: www.elsevier.com/locate/jenvrad

Estimating the terrestrial gamma dose rate by decomposition of the ambient dose equivalent rate

P. Bossew [a, *], G. Cinelli [b], M. Hernández-Ceballos [b], N. Cernohlawek [c], V. Gruber [d], B. Dehandschutter [e], F. Menneson [e], M. Bleher [a], U. Stöhlker [a], I. Hellmann [a], F. Weiler [a], T. Tollefsen [b], P.V. Tognoli [b], M. de Cort [b]

[a] German Federal Office for Radiation Protection (BfS), Berlin, Munich, Freiburg, Germany
[b] European Commission, DG Joint Research Centre (JRC), Institute for Transuranium Elements, Ispra, Italy
[c] Austrian Federal Ministry of Agriculture, Forestry, Environment and Water Management, Vienna, Austria
[d] Austrian Agency for Health and Food Safety (AGES), Vienna and Linz, Austria
[e] Belgian Federal Agency for Nuclear Control (FANC), Brussels, Belgium

ARTICLE INFO

Article history:
Received 5 November 2015
Received in revised form
11 February 2016
Accepted 13 February 2016
Available online 28 February 2016

Keywords:
Ambient dose equivalent rate
Terrestrial gamma radiation
Time series

ABSTRACT

An extensive network of dose rate monitoring stations continuously measures ambient dose rate across Europe, as part of the EURDEP system. Its purpose is early warning in radiological emergencies and documenting its temporal and spatial evolution. In normal conditions, when there is no contribution to the dose rate signal coming from fresh anthropogenic contamination, the data represent the radiation "background", i.e. the combined natural radiation and existing anthropogenic contamination (by global and Chernobyl fallout). These data are being stored, but have so far not been evaluated in depth, or used for any purpose. In the framework of the EU project 'European Atlas of Natural Radiation' the idea has emerged to exploit these data for generating a map of natural terrestrial gamma radiation. This component contributes to the total radiation exposure and knowing its geographical distribution can help establishing local 'radiation budgets'. A further use could be found in terrestrial dose rate as a proxy of the geogenic radon potential, as both quantities are related by partly the same source, namely uranium content of the ground. In this paper, we describe in detail the composition of the ambient dose equivalent rate as measured by the EURDEP monitors with respect to its physical nature and to its sources in the environment. We propose and compare methods to recover the terrestrial component from the gross signal. This requires detailed knowledge of detector response. We consider the probes used in the Austrian, Belgian and German dose rate networks, which are the respective national networks supplying data to EURDEP. It will be shown that although considerable progress has been made in understanding the dose rate signals, there is still space for improvement in terms of modelling and model parameters. An indispensable condition for success of the endeavour to establish a Europe-wide map of terrestrial dose rate background is progress in harmonising the European dose rate monitoring network.

1. Introduction

Across Europe, more than 4500 stations continuously monitor ambient equivalent dose rate. They belong to nation monitoring networks and are operated by national authorities responsible for radiation protection. Together, these networks contribute to the EURDEP system, run by the Joint Research Centre (JRC) of the European Commission.[1] The purpose of the networks and of the EURDEP platform is early warning in radiological emergencies. The data are transferred in almost real time to national and European central servers and are available to the public via an internet page, https://eurdep.jrc.ec.europa.eu/.

The national networks differ in design, as a consequence of different approaches and policies. This complicates joint interpretation of the data. Work aimed to understand the differences and to attempt posterior (or "top down") harmonization by application of harmonization algorithms to the individual results has been an

* Corresponding author.
[1] more precisely, by the REM group, part of the JRC's Institute for Transuranium Elements, https://rem.jrc.ec.europa.eu/RemWeb/Index.aspx. EURDEP also includes networks of stations for monitoring airborne contamination.

http://dx.doi.org/10.1016/j.jenvrad.2016.02.013
0265-931X/

issue for more than 10 years at the JRC in the framework of the AIRDOS project and related research activities.

No radiological event detectable by the dose rate networks has occurred in Europe since the Chernobyl accident in 1986. The dose rate generated by the Fukushima cloud and subsequent fallout over Europe was about three orders of magnitude below the detection capabilities of the monitors that contribute to EURDEP. Still, data are being collected and stored in routine or background mode. They reflect essentially the natural radiation background. So far, little use has been made of these data. Although made for a different purpose, the data could however be of scientific use. One is the European Atlas of Natural Radiation, which has been under development since 2006 at the JRC, and which will be a collection of maps, including terrestrial gamma dose rate, among others (De Cort et al., 2011; Cinelli et al., 2015). A second possible use is terrestrial gamma dose rate as predictor of the geogenic radon potential (Cinelli et al., 2015; Bossew et al., 2015a,b). In an ambitious first attempt, Szegvary et al. (2007a) generated a terrestrial gamma dose rate map of Europe. Here we refine that analysis. Uses that have been suggested are estimating soil humidity and radon flux from the ground (Szegvary et al. (2007b) and Stöhlker et al. (2012)).

The recorded ambient dose rate has several components, which have to be separated in order to recover the terrestrial gamma component. Among these components are the intrinsic background or self-effect, the contribution of secondary cosmic rays and other minor contributions. The terrestrial background consists of the gamma dose rate produced by U and Th decay series and ^{40}K concentration in the ground, and of an anthropogenic contribution from global and Chernobyl fallout. In addition, rain and snow can cause precipitation of Rn progenies on the ground, which can generate short-lived peaks of relatively high ambient dose rate (called Radon (Rn) peaks).

In this article, we describe the decomposition of ambient dose rate in more detail. In particular, we present three algorithms aimed to separate the Rn peaks from the remaining terrestrial components. So far (autumn 2015), the analyses were performed for German, Austrian and Belgian dose rate monitoring stations. We also discuss properties of that terrestrial background which is, to some extent, temporally variable due to environmental conditions related to meteorology. A relatively complicated problem, also addressed, is estimation of the anthropogenic (fallout) component. We give examples of decomposed dose rate time series. Finally, we discuss uncertainties involved in the procedure.

This paper is devoted to methodological aspects. Detailed statistical evaluation and discussion of the data of all investigated stations, as well as mapping of terrestrial dose rate, will be presented in a future article.

2. Ambient dose equivalent rate

2.1. Definition

The ambient equivalent dose H*(10) is a measurable equivalent of the effective dose, which quantifies the risk to human health associated to radiation exposure. For its exact definition see ICRU-51 or IAEA.[2]

In the following we use the symbol H* as abbreviation for ambient dose equivalent rate, dH*(10)/dt, for simplicity.

The dose rate probes must be calibrated to yield H* values for usual environmental radiation fields within some tolerated uncertainty. Calibration and quality assurance of dose rate monitors are rather complicated subjects, not to be discussed here. Given its practical importance, quality assurance of dose rate metrology, in particular with respect to harmonising national European networks, is subject to great efforts. As example we want to mention the long-term experiment for intercomparison of monitors under real ambient conditions INTERCAL (Bleher et al., 2014). In Europe they are mainly coordinated by EURADOS (European Radiation Dosimetry) working group 3, e.g. Wissmann and Sáez-Vergara (2006), Sáez-Vergara et al. (2007), Dombrowski et al. (2009) and Neumaier and Dombrowski (2014).

2.2. Components

Let H*(source; true) be the true ambient dose equivalent rate from a source. Generally the total dose rate H*(true) can be decomposed into the following components:

$$H*(\text{true}) = H*(\text{cosm}; \text{true}) + H*(\text{air}; \text{true}) + H*(\text{terr}; \text{true}),$$

where H*(cosm; true) is the contribution from cosmic rays, H*(air; true) the one of radionuclides in air and H*(terr; true) terrestrial radiation from gamma emitters in the ground and on the ground surface. The terrestrial component, in which we are interested here, can in principle be recovered by subtracting the other components from measured H*. However, the true dose rate is not known, but only one measured or observed by a detector. The relationship between true and observed dose rate is not trivial, as will be discussed in the following sub-section.

Here we restrict discussion to “background situations”, i.e. if no anthropogenically contaminated air is present. Also signals due to activities such as nearby material testing using gamma sources, are excluded in this analysis. Also external contamination of the detector housing seems negligible even in the case of anthropogenic fallout (C. Debayle, personal communication). Pending further information we assume the same for Rn progenies attached to the detector housing.

An overview on physical effects that are visible in the recordings of the German dose rate network is given in http://odlinfo.bfs.de/interpretation.php?lang=EN. Detailed analyses can be found, e.g., in Smetsers and Blaauboer (1994, 1997a,b).

2.2.1. True and observed dose rate

The detector responds to radiation with true dose rate from a source with a count rate N (measured, e.g., in cps), which is a function of the dose rate corresponding to the arriving photon flux and the energy of the radiation. Let N (source) be the detector response,

$$N(\text{source}) = f_{\text{source}}(H^*(\text{source}; \text{true})),$$

f_{source} – the source-specific response function. Detectors are designed to guarantee linear response as accurately as possible, i.e.

$$N(\text{source}) = N_0 + R_{\text{source}} H^*(\text{source}; \text{true}),$$

R_{source} – the response factor to the source with certain energy or energy mixture. The null-count rate N_0 is source-independent, but depends on intrinsic properties of the detector.

In the calibration procedure, a calibration factor k_{source} is determined such that for a certain type of source, the product

$$H^*(\text{source}; \text{observed}) = K_{\text{source}} N(\text{source})$$

equals H*(source; true). Since the response of the detector depends

[2] https://www.iaea.org/ns/tutorials/regcontrol/intro/glossaryi.htm, https://www.iaea.org/ns/tutorials/regcontrol/intro/glossaryd.htm#D57.

on source energy, a calibration factor k_{source} applied on the detector response to a source with different gamma energy, N (source') = $N_0 + R_{source'}$ H*(source'; true), i.e.

$$H^*(\text{source}';\text{observed}) = K_{source} N(\text{source}')$$

is different from H*(source'; true), in general.

Ambient dose rate detectors shall be designed such that the observed dose rate equals the true one in good approximation for source energies that are characteristic for gamma energies deemed relevant for radionuclides released by nuclear accidents. These are mostly in the range between 100 and 1000 keV.

Thus, if one succeeds in designing the detectors such that the dependence of their response factors on gamma energy is about constant in this energy range, the observed dose rate is about equal the true one, if the detector has been calibrated with a source whose energy is in that energy range. This can indeed be achieved in good approximation; two examples are shown in Fig. 1 for the detectors used in the Belgian and in the Austrian early warning networks. The graphs give the response relative to ^{137}Cs. Linearity is approximately given between 100 and 1000 keV.

Geogenic radionuclides of the ^{238}U and ^{232}Th series have most gamma energies in the same range, except for a few high-energy gamma lines (1764 keV from ^{214}Bi/^{238}U series, 2615 keV from ^{208}Tl/^{232}Th series and 1461 keV from ^{40}K).

There seems to be a tendency to use radium instead of ^{137}Cs sources for calibrating ambient dose rate detectors, which somewhat mitigates that problem that the high energy gamma lines lead to overestimation of the terrestrial component. The German IMIS detectors are calibrated with Ra sources.

As a summary, common detectors designed for measuring ambient dose rate from anthropogenic fallout yield estimates of the terrestrial dose rate, which are sufficiently accurate for many purposes, including that which we have in mind in this study.

Denoting the actual calibration factor k (usually for ^{137}Cs or ^{226}Ra and progenies), the observed dose rate from all sources equals

$$H^*(\text{observed}) = k(N_0 + R_{cosm}H^*(\text{cosm};\text{true}) + R_{air}H^*(\text{air};\text{true}) + R_{terr}H^*(\text{terr};\text{true})),$$

assuming that a common R_{terr} for natural and anthropogenic radionuclides is applicable with tolerably small inaccuracy. We shall see that H*(air) from natural radionuclides contributes little; it will therefore not be further discussed.

Since, from the logic of calibration, k $R_{terr} \approx 1$, and defining k N_0 = H*(self), the self-effect in terms of the quantity H*(10), we see that approximately, the terrestrial contribution to dose rate can be calculated by,

$$H*(\text{terr}) \approx H*(\text{observed}) - H*(\text{self}) - R_{cosm}\,H*(\text{cosm};\text{true})$$

Important parameters, in our context, are therefore H*(self) and R_{cosm}, which are detector specific and must be determined by experiments.

2.2.2. Self-effect

The self-effect (also called intrinsic background, zero- or null-effect) results from radionuclides in the structural materials of the detector and from electronic noise. It varies between detector types and also between specimens of the same probe. It can be determined in underground salt mines where radiation background is very low (e.g., Wissmann 2006, Wissmann et al. 2007).

- The German ambient dose rate measuring stations, run by the German Federal Office for Radiation Protection (BfS), which deliver data into the IMIS system[3] and in turn contribute to EURDEP, use GS-05 Geiger-Müller (G-M) probes and follow-up models (currently GS-07). Each probe is characterized individually. Before transmission to EURDEP, the self-effect is subtracted.
- The Austrian SFWS network[4] uses proportional counters RS-03 from Bitt Technology.[5] A generic value of the self-effect is subtracted. For the remaining or residual self-effect we use H*(self) = 2 nSv/h, although experiments performed on two probes suggest an even lower value of about 1.1 nSv/h (Sáez-Vergara et al., 2007, table 2). Austrian data transmitted to EURDEP include only the residual self-effect.
- For the Belgian network TELERAD[6] consisting of G-M probes Envinet IGS 411[7], the residual self-effect after subtraction of a

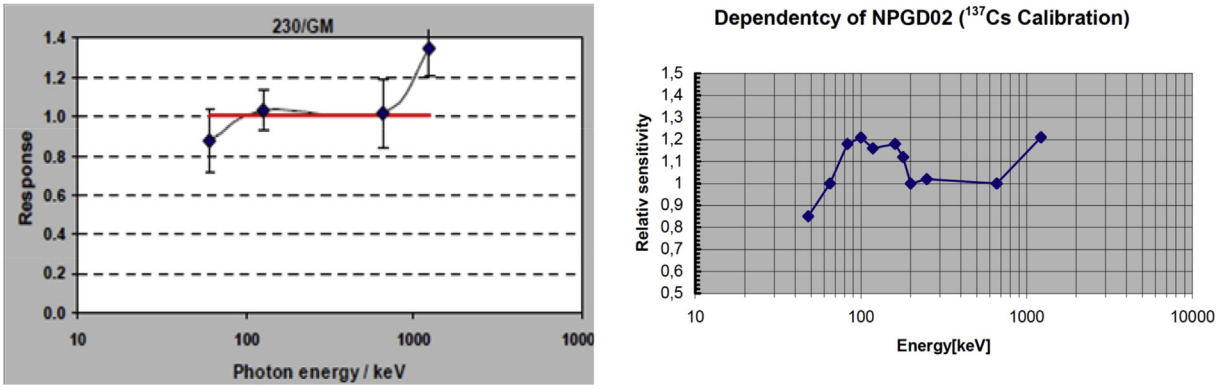

Fig. 1. Energy responses relative to ^{137}Cs of two dose rate detectors: Left: Envinet IGS 411 B–H G-M-counter, used in the Belgian early warning network; taken from Menneson et al. (2015). Right: Bitt RS-03 proportional counter, used in the Austrian early warning network; taken from MANUAL GAMMA DETECTOR RS03/X V.1.9 short (2005).

[3] http://www.bfs.de/EN/topics/ion/accident-management/measuring-network/imis/imis.html, http://odlinfo.bfs.de/index.php?lang=EN, http://80.153.15.213/broschuere_en.html.

[4] http://www.bmlfuw.gv.at/umwelt/strahlen-atom/strahlenschutz/strahlen-warn-system/sfws.html (in German only).

[5] http://www.bitt.at/en/products/gamma-detector/rs04-x.

[6] http://telerad.fgov.be/(French and Flemish available).

[7] http://envinet.com/english/igs-gammadetector/igs411.

generic mean equals 0.9 ± 1.51 nSv/h (Menneson et al., 2015). Also here, data are transmitted to EURDEP including only the residual self-effect.

Experiments with a subset of German GS-05 probes have shown about 7% variability (1σ) between probes of the same model. Evaluation of all GS-07 probes gave a population variability of 20% (1σ).

2.2.3. Cosmic radiation

At altitudes up to above 10 km above sea level cosmic radiation consists mainly of secondary cosmic radiation (SCR), which is generated by interaction of primary radiation (mainly protons) with atoms of the atmosphere. It consists mainly of muons, in addition to electrons, positrons, neutrons and gamma rays. For the physical background and details, see e.g. Wissmann et al. (2005), and references therein. According to Wissmann and Sáez-Vergara (2006), at low altitudes muons contribute about 50% to the dose rate, neutrons 20%, gamma rays less than 2%. According to Bouville and Lowder (1988), muons contribute two-thirds. Different types of detectors respond differently to SCR. G-M and proportional counters, calibrated to typical environmental gamma radiation spectra (usually with ^{137}Cs or ^{226}Ra sources) overestimate SCR, while scintillators are marginally sensitive to SCR. For exact measurement of the SCR, ionisation chambers, muon and neutron detectors are used.

The intensity and energy spectrum of SCR at a detector depends on the attenuation by the mass of air lying above the detector. Air mass depends on altitude above sea level and actual weather. Since air pressure depends on the air mass, it can be used as proxy to quantify attenuation of SCR. Thus, for exact purposes, one defines the barometric altitude, which is derived from measured air pressure by applying a standardization model (e.g. Wissmann et al., 2007). Here, for practicality, we use the topographic altitude instead. The error is considered negligible for our purposes.

The standard reference for altitude dependency of SCR seems to be Lowder and O'Brien (1972). The graphs shown in Fig. 2 were created from the data of that report. (However, in that report, dose equivalent refers to something like H*(5) instead of the modern standard H*(10).) One can notice an additional but weak dependence on geographical latitude and solar cycle. The graph also shows measured values taken from Wissmann et al. (2007; table 4), obtained with an RS-131 ionization chamber (except the values for 33 and 35 m altitude, by MUDOS muon detector). The measurements labelled "Wissmann-RSS" were performed between 2003 and 2006, which was a time of mean solar activity.

For the variation with solar cycle and for the latitude band given in Lowder and O'Brien (1972), their data show a range of about 5–20 nSv/h, or relative range (range/arithmetical mean) between 12% and 17%, for low and high altitudes, respectively. Thus, if latitude (in this band) and position within the solar cycle are not known, this limits the accuracy with which the true SCR dose rate can be estimated from the graph.

For the German GS-05 probes, the altitude dependence of SCR has been determined experimentally. In Wissmann et al. (2007; table 4, last column) values of the estimated true cosmic dose rate are given. Converting this into hypothetical observed dose rate, assuming the detector was calibrated with a ^{226}Ra source, i.e. multiplying the values by 1.36 ± 0.04 (mean value of R_{cosm}, ibid. table 2), gives the values plotted as crosses in Fig. 3. Uncertainty is reported as about 5%, including the one of R_{cosm} (Ra) leads to 6–7%. (For the purpose of that paper, the authors assumed values of R_{cosm} independent of altitude. Since the energy of SCR varies with altitude, so in reality does R_{cosm}, as the authors also note in the article.)

For comparison, Fig. 3 also shows the results from three approximations. The curve labelled "GS-05 AIRDOS" comes from that report (AIRDOS (n.y.), sec. 3.2.2.1),

$$H^*(\text{cosm; observed})(h) = 41.71 + 1.131 \times 10^{-2} \times h - 2.08 \times 10^{-6} \times h^2 + 1.9 \times 10^{-9} \times h^3,$$

H^* in nSv/h and altitude h in m. In the AIRDOS report this was cited as absorbed dose rate, which seems to be an error. Another approximation has been suggested by U. Stöhlker (personal communication),

$$H*(\text{cosm; observed})(h) = 42 \exp\left(3 \times 10^{-4} \times h\right)$$

Murith and Gurtner (1994) give a similar approximation,

$$H^*(\text{cosm; observed})(h) = 37.0 \exp\left(3.8 \times 10^{-4} \times h\right)$$

also apparently for G-M probes; same in Rybach et al. (1997) and in the following referred to as "Rybach formula". Both formulae are also displayed as curves in Fig. 3. As can be seen, data and approximation formulae correspond reasonably well within about 10% tolerance.

For the Belgian detectors a similar dependence as for the German ones can be assumed, since they are both G-M probes with

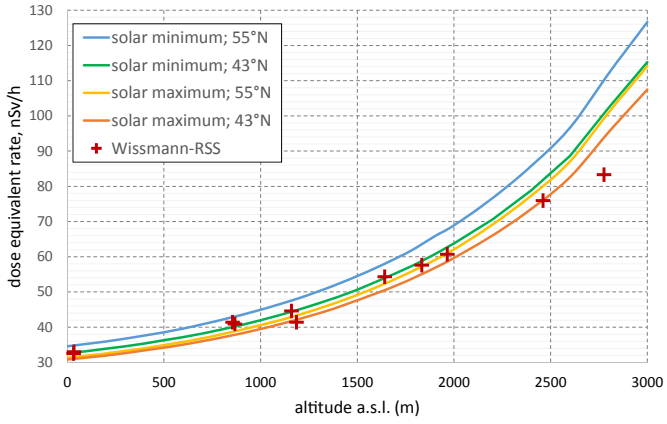

Fig. 2. Dependence of estimated true cosmic dose equivalent rate on altitude. The data for the curves labelled solar minimum and maximum and 2 latitudes were taken from Lowder and O'Brien (1972), table 2. In addition, measured values from Wissmann et al. (2007) are shown.

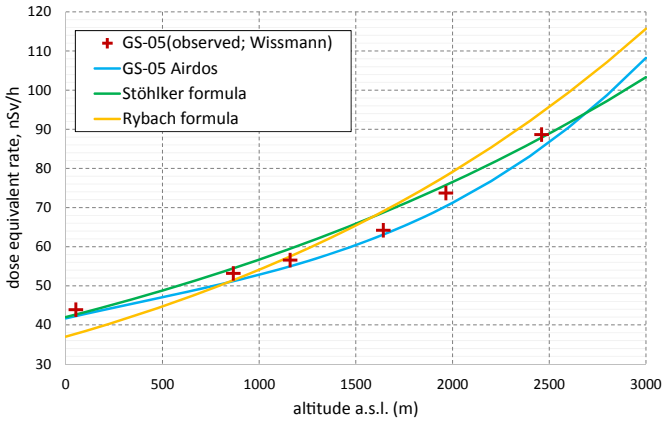

Fig. 3. Dependence of observed cosmic dose equivalent rate on altitude and comparison with approximations from different references (see text).

similar dimensions. At present, we have no information about SCR dependence on altitude for the Austrian detectors (proportional counters). Pending better data, we estimated dependency by a default average formula, calculating the arithmetic mean of the AIRDOS, the Stöhlker and the Rybach formulae. The relative range between the three formulae is between 6% and 12% (lowest for altitudes about 800 m), i.e. roughly similar to the one of the observations (red crosses in the graph, Fig. 3). Therefore, for G-M counters not too different from GS-05, and accounting for solar cycle and latitude effect, we should count with an uncertainty of about 15% when estimating the SCR component of the ambient dose rate, possibly more for high altitudes. Performing experiments at high-altitude stations could help to reduce uncertainty.

In future research, knowledge of dependence of SCR on altitude of different detector types and models should be improved. Once the missing information is available, we shall redo the analyses with improved parameters for cosmic response.

Response of a G-M counter to SCR depends on detector geometry. In particular, the sensitivity is different if a detector in the shape of a long tube (as common in ambient dosimetry) operates vertically (the standard) or horizontally. A thorough discussion can be found in Spiers et al (1981; section 3.1.3).

2.2.4. Natural radionuclides in air

Airborne gamma radiation which can be recorded by an ambient dose rate detector can have the following sources: Rn progenies in the atmosphere and gamma radiating cosmogenic radionuclides such as ^{7}Be or ^{22}Na.

For ^{7}Be and ^{22}Na, available data about concentration in air and about deposition on the ground, as well as dose conversion factors for immersion and ground shine lead to the conclusion that resulting contributions to the ambient gamma dose rate are very small, far below 1 nSv/h.

The dose rate originating from Rn progenies evidently depends on their distribution in the atmosphere. As a generic value Smetsers and Blaauboer (1997a) proposed 0.50 (nSv/h)/(Bq/m^3) for EEC concentration. For Germany, long-term mean outdoor Rn concentrations vary between 3 and 31 Bq/m^3, with arithmetic mean (AM) 9.5 Bq/m^3 and standard deviation (SD; describing the geographical variability; there is a significant geographical trend) 5.1 Bq/m^3. The equilibrium factor has been estimated as 0.5 (Kümmel et al., 2014). Similar values have been reported by other authors. Using the above conversion factor, 10 Bq/m^3 would contribute with about 2.5 nSv/h.

2.2.5. Terrestrial radiation – anthropogenic sources

Gamma radiating radionuclides deposited on the ground by fallout contribute to the terrestrial gamma background. In Europe, sources are ^{137}Cs from global and Chernobyl fallout. Global fallout is relatively uniformly distributed with inventories in the order of a few kBq/m^2. Chernobyl fallout varies across Europe (De Cort et al., 1998) between less than 1 kBq/m^2 up to >100 kBq/m^2 in parts of Scandinavia, the Alpine and pre-Alpine region, and up to some MBq/m^2 locally in regions of Ukraine, Belarus and Russia around the Chernobyl NPP. Certainly except these regions which were more strongly affected than most of Europe, the contribution of global and Chernobyl fallout to the terrestrial dose rate is small, 30 years after the accident (26 May 1986).

A number of authors have discussed the ambient dose rate above ground for differently contaminated soil. Factors which affect the dose rate conversion factor $\Gamma = H^*(10)/J$, J the radionuclide inventory in soil, Bq/m^2, derive from scattering and attenuation in soil and air. Specifically, these are depth profile of radionuclide concentration, chemical composition of soil and humidity. For "fresh" superficial fallout on an ideal plane, $\Gamma = 3.0$ (nSv/h)/(kBq/m^2) can be inferred from the classical report by Beck et al. (1972). Zähringer and Sempau (1997) give a value of 3.09 (nSv/h)/(kBq/m^2) (converted from air kerma to ambient dose equivalent rate with 1.2 Sv/Gy), Lemercier et al. (2008) also found 3.09 (using a gamma yield of ^{137}Cs of 85%), and Saito and Petoussi-Henss (2014), 3.15 (nSv/h)/(kBq/m^2).

A number of authors studied the influence of distribution of the source in the ground, of the chemical composition of soil and surface roughness, not to be further reviewed here. During the Austrian Chernobyl survey, Bossew et al. (2001) found a "realistic" $\Gamma = \sim 1$ (nSv/h)/(kBq/m^2) by regression analysis of measured dose rate against activity concentration values. This can be understood as a rough average value over many different locations of "typical" undisturbed meadows, which have different soil type, climate, surface roughness (micro-relief, grass) and several years of migration of the fallout into the soil.

The contribution of this radiation source to the terrestrial dose rate is difficult to estimate, unless site-specific data are available. In Germany, the monitoring stations have been characterized by in situ gamma spectrometry; from the spectra, dose rates pertaining to individual radionuclides can be estimated. Further evaluation of this data is planned.

If such data are not available, as for most networks, contribution of ^{137}Cs could be estimated very roughly as follows. The geographical distribution of fallout is known, however with different resolution in different parts of Europe (De Cort et al., 1998). From the available point data the ^{137}Cs inventory at the site of a monitoring station can be interpolated by means of geostatistical methods, in principle. The problem is however twofold: (1) it is in general not known whether the ground has been left undisturbed since fallout, or whether it has been reworked or landscaped. In this case the actual ^{137}Cs inventory may be very different from the theoretical one; and (2) even if the location has been left undisturbed, the dose rate depends on the depth distribution of the contaminant, which is not known in general. Generic values based on knowledge of Cs migration in soil of different type could be used, but evidently, estimating local Cs migration rate involves high uncertainty.

2.2.6. Terrestrial radiation – natural sources

Terrestrial exposure to gamma rays above ground is generated by natural radionuclides present in all rocks and soils. The most important are ^{238}U and progenies, ^{232}Th and progenies and ^{40}K. Others such as the ^{235}U chain and even less, gamma emitting radionuclides of trace elements such as ^{138}La and ^{176}Lu do not contribute to a relevant extent.

Dose conversion factors are determined by Monte Carlo simulation of photons under defined conditions of interaction with soil matter. Homogeneous distribution in soil is assumed. (Practically all radiation comes from the upper 50 cm, see Gasser et al. (2014).)

Dose conversion factors differ remarkably between authors,

Table 1
Dose conversion factors for natural radionuclides homogeneously distributed in soil. Unit (nGy/h)/(Bq/kg).

Author	^{238}U series	^{232}Th series	^{40}K
Beck et al. (1972)	0.430	0.666	0.0422
ICRU-53 (1994)	0.462	0.604	0.0417
Saito and Jacob (1995)	0.463	0.604	0.0417
Clouvas et al. (2000)	0.399	0.544	0.0399
Quindos et al. (2004)	0.455	0.584	0.0429
Lemercier et al. (2008)	0.450	0.599	0.0427
Gasser et al. (2014)	0.357	0.482	0.036
Malins et al. (2015a,b)	0.444	0.592	0.042

perhaps due to different nuclear decay data and soil compositions used; for further discussion, see Gasser et al. (2014). Some values are tabulated in Beck et al. (1972), Saito and Jacob (1995), Clouvas et al. (2000), Quindos et al. (2004), Lemercier et al. (2008) and latest, to our knowledge, Gasser et al. (2014) and Malins et al. (2015a, b), who disputed the values of Gasser as methodically biased. An overview is given in Table 1. The values of Quindos et al. (2004) were determined experimentally. Clouvas et al. (2000) compared the results from different Monte Carlo codes.

In terms of ambient dose equivalent rate H*(10), Lemercier et al. (2008) find 0.564, 0.749 and 0.0512 (nSv/h)/(Bq/kg) for the ^{238}U series, the ^{232}Th series and ^{40}K, which corresponds to Sv/Gy ratios 1.253, 1.250 and 1.199, respectively. These ratios slightly depend on energy. Thus, the common conversion 1.2 Sv/Gy between absorbed dose and H*(10) is also approximately applicable for natural radionuclides.

In real soils the radionuclides are often not homogeneously distributed, in particular not so in undisturbed soils. Also, decay products of exhaled Rn and Tn can accumulate near the surface leading to higher estimations of U or Th concentration than actually present. Meteorological conditions influence attenuation of gamma rays (via humidity) and Rn transport; see e.g. the study of Lebedyte et al. (2003). Finally, micro relief and surface roughness (vegetation) of real grounds attenuates the gamma rays compared to ideal plane ground condition.

2.2.7. "Radon peaks"

Rn and its progenies exhaled from the ground disperse in the atmosphere until many km of altitude. The distribution profile depends on atmospheric and meteorological conditions and can be complicated. Precipitation (rain, snow, fog) leads to accumulation of Rn progenies on the ground surface due to washout (particles below the rain clouds) or rainout (scavenging within the clouds). The deposited gamma-emitting Rn progenies (mostly ^{214}Pb and ^{214}Bi) lead to enhanced terrestrial ambient dose rate, up to 300 nSv/h H*(10). The mechanism is complex, and in consequence so is the relation between dose rate, precipitation intensity, altitude and volume of clouds and concentration profile of Rn progenies in the atmosphere. Longer duration of precipitation does not lead to higher dose rate, because the atmosphere is cleaned quickly and supply of exhaled Rn to higher atmospheric layers is comparatively slow. Because of the short half-lives of ^{214}Pb and ^{214}Bi, 26.8 and 19.9 min, respectively, the dose rate peaks disappear relatively quickly due to the decay of these radionuclides. An example plot of dose rate and short precipitation episodes is shown in Fig. 4. The "Rn peaks" can be high enough to exceed notification and alarm levels and trigger verification procedures to check the cause of the dose rate increase. Algorithms for automatic identification of such events have been implemented to avoid first-kind errors (false alarms) in radiological alarm networks (see section 2.4).

For details see Smetsers and Blaauboer (1997a), Stöhlker and Bleher (2007) (deliverable 5–2) or Mercier et al. (2009).

2.3. Temporal variability

As has become clear in the previous paragraphs, ambient dose rate series are subject to fluctuations exceeding those induced by counting statistic. They are caused by natural phenomena and complicate the recognition of signals related to anthropogenic signals, which is the objective of early warning networks. Natural fluctuations can cause false alarms, but more importantly, small anthropogenic signals could pass undetected, concealed by the natural fluctuations (second kind error or false non-detection). Understanding the fluctuations is therefore important for optimal operation of the networks. Of course, second-kind errors are a negligible problem in the presence of strong signals, such as from the Chernobyl accident. Fig. 5 shows two time series from Austrian stations recorded after the Chernobyl accident. The arrival time of the contaminated cloud is easily recognizable. In this case the passing cloud left fallout, recognizable by the slowly decaying tail after the sharp rise, generated by radionuclides deposited on the ground. In the German network, the rate of false alarms is reduced by allowing generation of internal alerts only if at least two probes less than 30 km apart report signals above notification threshold within 1 h (For newer systems, there are efforts to implement an algorithm for generation of internal alerts by only one station.) For in-depth discussion and frequency of such events, see Stöhlker and Bleher (2007). Note that such a procedure requires comparability of the response of probes to dose rate signals, see section 2.5.

Fluctuations stemming from different physical causes have

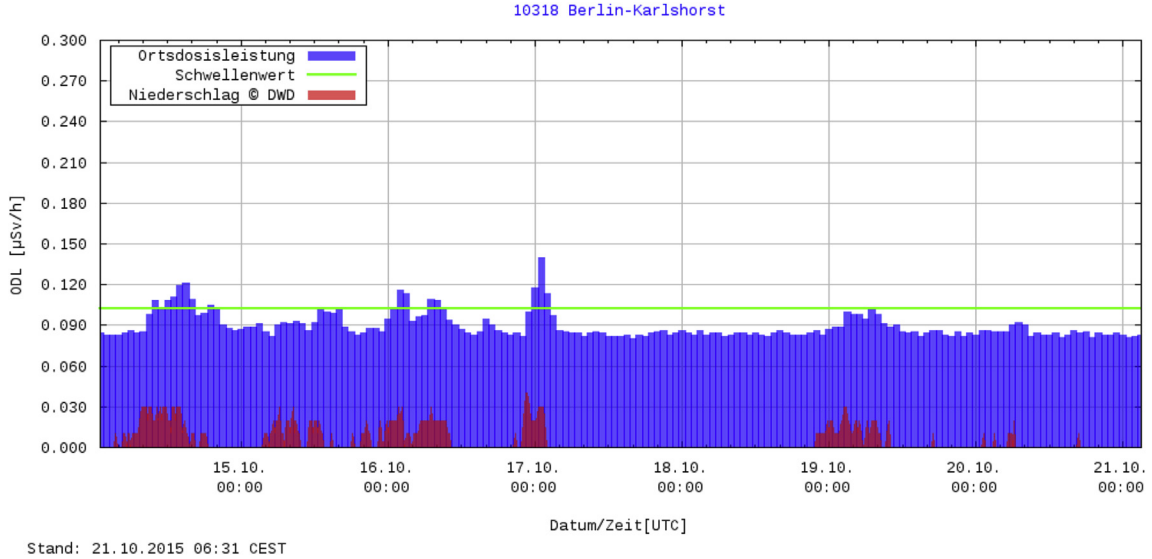

Fig. 4. Time series of ambient dose equivalent rate, recorded during 1 week at the BfS office in Berlin. Blue: dose rate; red: precipitation (radar data); green line: notification threshold. Fromhttp://odlinfo.bfs.de/index.php?lang=EN (For interpretation of the references to colour in this figure legend, the reader is referred to the web version of this article.)

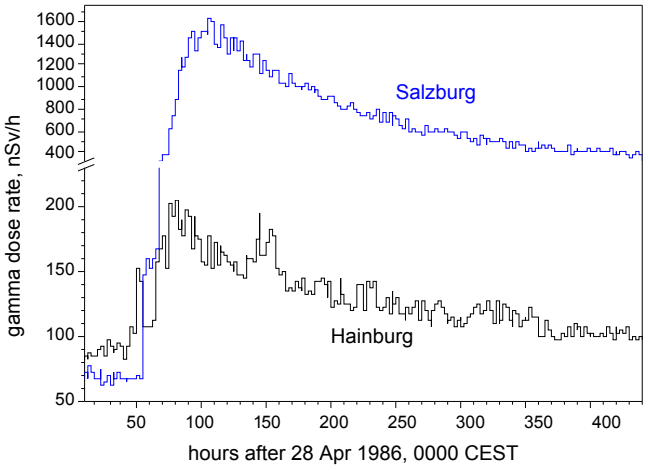

Fig. 5. Dose rate signal after the Chernobyl accident recorded by the Austrian Early warning network SFWS, at two locations. Temporal resolution: 2 h.

different patterns, in general. They are very different from an anthropogenic fallout-type signal, Fig. 5. Their temporal pattern or "signature" helps distinguishing them. Characteristic parameters are time scale, i.e. typical duration, periodicity and autocorrelation, i.e. the degree of statistical association between subsequent records. A summary is given in Table 2.

In our context, fluctuations of the terrestrial component deserve particular discussion. While the concentration of primordial natural radionuclides (^{40}K, ^{238}U, ^{232}Th) remains constant in the time scale used, this is different for their progenies. Depending on soil water content, Rn can migrate upwards with variable efficiency and thus the concentrations of its gamma radiating decay products close to the soil surface can vary.

Also for constant source activity, humidity influences the gamma ray flux above ground due to different attenuation by soil water. In dry periods, enhanced ambient dose rates can often be observed.

The "geophysical effects" include tidal forces (periodic; hours), stress changes in the earth mantle and crust (no further information available; but known to influence Rn transport and exhalation), and changes in the ground water table (some periodic, some erratic). A fluctuating ground water table can act like a pump on Rn transport and cause similar effects. (We thank one reviewer for suggesting to include these effects.)

Put together, the effects are complex and therefore difficult to model. Lebedyte et al. (2003) show the dependence of dose rate on monthly mean air temperature, on the thickness of snow cover (response of different detectors also shown in Bleher et al., 2014), on freezing depth and on Rn concentration in ground air. Meteorological conditions significantly influence Rn exhalation from soil, which contributes importantly to the dose rate fluctuations. Correlation between soil humidity and dose rate has been shown in Stöhlker et al. (2012).

Temporal fluctuations of the SCR due to meteorological factors and solar effects are discussed in Wissmann (2006).

2.4. Definition of the terrestrial background

After removal of self-effect and mean SCR dose rate, short-term fluctuations and short-term peaks ("low pass filtering"), a dose rate time series consists of contributions from terrestrial gamma radiation only (neglecting the "minor" contributions and residual SCR fluctuations). As explained, this is not a constant, but slightly variable value. To summarize, its causes are (typical times in brackets):

- Soil humidity effects: Variable attenuation of gamma rays and depletion or accumulation of Rn/Tn progenies near the surface (days, weeks).
- Snow effect (days to months).
- Residual uncertainties from Rn peak removal (hours).
- Residual variability of SCR, which has been assumed a site specific constant (hours to many years).
- "Minor" contributions: Rn progenies in air (hours, daily and seasonal cycles).

If the terrestrial component of a dose rate series measured for one year or longer is analysed, the effects are "averaged away", except the one due to the solar cycle. Apart from this, 1- or more-year averages calculated from different time intervals can still be different, because the factors – in particular snow and humidity effects – are seasonally recurring, but not regular in duration and extent.

Therefore, while the straightforward definition of the terrestrial dose rate background (BG) at a site would be the average of the terrestrial component as estimated above, a definition which is less prone to variability due to environmental effects which are different from year to year, could be averaging only values of the terrestrial component except episodes of snow or particularly dry soil. One may argue, on the other hand, that these effects are typical for a site and its dose rate characterization should therefore include their influence. Perhaps one would adopt different definitions for different purposes.

Below we shall discuss how the snow effect could be removed automatically.

Table 2
Temporal signature of dose rate signals.

Source	Temporal autocorrelation	Periodicity	Time scale
Counting statistic	No	No	Time scale of measurement, propagates into transmitted data
Rn peaks	Yes	No	Hours
Nuclear accidents	Yes	No	Hours to years, depending on half life of radionuclides involved and on exposure pathway (radiation from passing cloud or fallout on ground)
Snow cover	Yes	Yes, but irregular	~ weeks to months
Soil humidity	Yes	No	Days - weeks
Seasonal variation of SCR	Yes	Yes	Season (months)
Solar cycle	Yes	Yes	About 11 years
Geophysical effects	Yes	Some of them	Hours to weeks (?)
Detector re-calibration with radiation sources	Usually no	No	Maximally hours
System malfunctions	Sometimes	No	As long as not fixed

2.5. Data and site characteristic

The data of dose rate time series were retrieved from the EURDEP database. The series extended over about 1.5 years for Austria (mid-August 2013 to end-February 2015) and about 2 years for Belgium and Germany (mid-August 2012 to mid-August 2014). In addition, a few very-long-term series (>4 y) were analysed. The monitors which constitute the German network are described in more detail e.g. in Luff et al. (2014). No comparably detailed description exists for the Austrian and Belgian probes.

As this paper is devoted to methodology, no summary results over all stations will be presented here.

Although all dose rate signals of monitoring stations of early warning network (or any other ambient dose rate monitoring) contain a contribution from terrestrial radiation, not all can be used for estimating a value of that component, which is characteristic for the area. With this term, we understand the terrestrial radiation from characteristic ground, which means:

- Natural ground, not altered by material from other regions.
- The natural terrestrial radiation should come only from the ground, but not from buildings or road or water surfaces etc.
- Radiation from ground should not be attenuated by objects close to the detector, such as trees.

Similar conditions apply to anthropogenic radiation, whose detection is the primary purpose of early warning networks. This has led to defining standard conditions for ambient dose rate monitoring stations. The ideal situation, a plane field of infinite extension, does not exist, but it can be approximated with tolerable uncertainty. Real monitoring stations have individual site characteristics, which describe the geometry of the location, i.e. its location in the surrounding near environment. Different networks have different policies in (a) selecting locations for monitors and (b) documentation of the sites. If the policy is that a monitor shall be able to detect an increase due to anthropogenic contamination of certain amount relative to its background, as for the Austrian early warning network SFWS, the site geometry does not matter too much; in particular monitors located on roofs are common (Relocation to sites whose characteristic is closer to the standard one, is under way.) Evidently, such probes register the radiation from building materials but not the one from characteristic ground. In Belgium and Germany, on the other hand, policy is that values should be comparable between stations, which implies that they are set in comparable site characteristic, in practice as close as possible to the standard. Deviations from the standard have been quantified in Germany for each station, allowing to quantify, subject to uncertainty induced by those deviations, dose rate signals with respect to a contamination level (Zähringer and Sempau, 1996, 1997).

For our purpose, the most important condition is that the monitors are located in sufficient distance from buildings and from roads. Fig. 6 shows the fraction of dose rate that comes from a disc of given radius around the monitor, for gamma emitters homogeneously distributed in the ground. (Note that the dose rate is also generated by the part of the energy spectrum below the full energy photo peak due to Compton scattering in soil, air, and backscattering (skyshine).) A similar graph has been shown in Malins et al. (2015a, b). We classified the suitability of locations for estimating the terrestrial background approximately according this dependence. The matter will be further discussed in a future article dealing with maps of terrestrial dose rate.

As not all monitoring stations comply sufficiently with the standard, as required for estimating a characteristic terrestrial background, only a subset of existing stations was selected. For Austria, Belgium and Germany, 80 (of about 320), 120 (of 128) and 1664 (of about 1800) were retained.

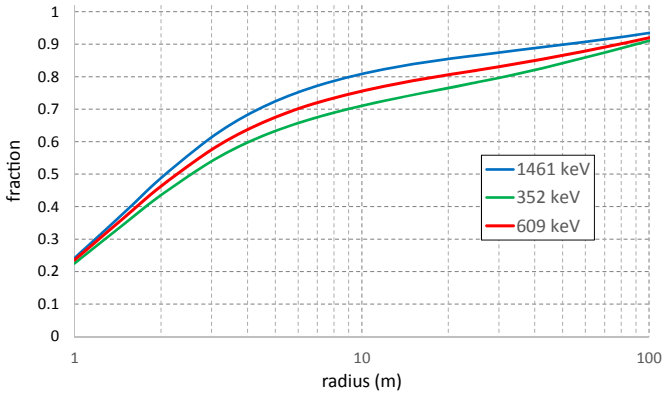

Fig. 6. Fraction of the dose rate coming from a disc of given radius around the detector, for three gamma energies characteristic for geogenic radionuclides; source homogeneously distributed in the ground. The detector is located 1 m above ground. From data in Zähringer and Sempau (1997), table 7.

It seems that mostly the probes are anchored in the ground by a concrete base plate, which can be a disk or square shaped concrete slab or block about 50 cm in diameter. In general its content of natural radionuclides is different from the surrounding ground. Therefore it will contribute a terrestrial gamma flux that is different from the one if the base was only natural ground. Given the small contribution from small radiuses (Fig. 6), the error induced this way is probably small, but exact investigation of the effect is missing, to our knowledge.

3. Decomposition algorithms

In the following, we present three methods to estimate the terrestrial gamma radiation background. All rely on analysing long time series, typically spanning at least 1 year, of records of ambient dose equivalent rate. The “zero-th” step in the analyses is inspection of the time series and pre-processing, if necessary. Series must be temporally ordered, and no systematic trends should be included due to factors related to the measurement process, such as, typically, generated by replacing the probe with a new one or relocation or physical or geometrical alteration of its site. These may have the effect of introducing a step in the series. Detecting such steps can be difficult if they are small and database records should be consulted. Also missing values due to interruption of operation may cause a problem in the algorithms.

As one step in all cases, self-effect and estimated cosmic contribution are subtracted. This can be done in the beginning or after having determined the gross average (in the peak − valley method, section 3.3). Since these are assumed constant contributions the sequence does not matter. The next step is removal of Rn peaks, which has been solved differently by the methods.

3.1. Median method

The first method among the three has been proposed by M. Bleher in 2009 (unpublished). Within moving time windows (length = 1 week), the median of the series data is computed. If less than half of the data in the window are “contaminated” ones, i.e. affected by Rn or other peaks, the algorithm yields stable location estimates of dose rate except these peaks. If there are no such peaks in the window, the result is the median of the data. If 50% minus one value are contaminated, the algorithm yields the maximum of

the remaining ones, i.e. of those, which constitute the background. This means that the algorithm yields slightly ill-defined estimates of location measures of the BG. In practice this is marginally relevant, however, and the results coincide well with the ones of the other methods. The method is implemented very easily and it is robust in most cases.

For the analyses performed here, the median method was used together with the following method and the window size was set to 20 days.

3.2. Iterative peak identification

Within a window of given length (20 days chosen), starting at the beginning of the series, arithmetic mean (AM) and standard deviation (SD) of the values are computed. Values > AM + α(remove) × SD are excluded (α(remove) = 1.65 chosen). The procedure is repeated until no more values are being excluded from the window. Note that only upwards extremes are removed. Then the window proceeds one time step ahead (1 day chosen), until the end of the series. Usually three or less iterations are required.

The algorithm assigns a value of the terrestrial BG to each time step (1 day), resulting in an estimate of a time series of the terrestrial BG, see the red lines in Fig. 8. As next step the AM over these values is calculated; this is defined as terrestrial BG dose rate.

3.2.1. Snow effect

An attempt has been made to automatically identify periods when the terrestrial BG is attenuated by snow. First, the maximum (max) of the terrestrial BG series is found. The values of the series are then divided, so that only values > max − incr are retained; increment 'incr' chosen small, here 0.1% of max. The coefficient of variation (CV) of the remaining values is computed. Then a second increment of same size is subtracted, thus including somewhat more values, and so on. The procedure is stopped if the CV reaches 4%, which has been found empirically as usual variability of the terrestrial BG, excluding the snow effect. That way the values are approximately divided into "no-snow" and "snow" periods. This procedure has worked well for Austrian data, but not so for the German ones. The reason seems to be that on some German locations there is a more significant "soil dryness effect", resulting in episodes with enhanced dose rate, inverse to the snow effect, invalidating the algorithm. A practical, i.e. simple solution is still to be found.

3.3. Peak - valley method

The proposed method is based on the identification of Rn (and its progenies) peaks and their corresponding preceding and following valleys. To identify the peaks, the 75th percentile (P75) is applied over the resulting smoothing original dose rate series, which is obtained applying the Moving Average filter (Tandon and Attri, 2011; Lee et al., 2012) of the four values in forward and backward direction from each original value. The P75 threshold is calculated yearly for each sampling station, taking as reference the yearly smoothed total-dose rate series, and it is based on the need of selecting not only the highest values that are usually related to extreme scenarios.

Once identified the peaks (red points in Fig. 7), the associating valleys are defined as the points with the lowest values (valleys – green points in Fig. 7) before and after the peak. Finally, the average of the set of valley points is obtained. From this value, to calculate the terrestrial gamma dose rate, the "constant" components are subtracted (estimated cosmic and internal BG). The program has been written in R code. For more information about this algorithm the reader is referred to Cinelli et al., 2014.

4. Results and discussion

4.1. Exemplary time series

Two examples of long-term dose rate series are shown in Fig. 8.

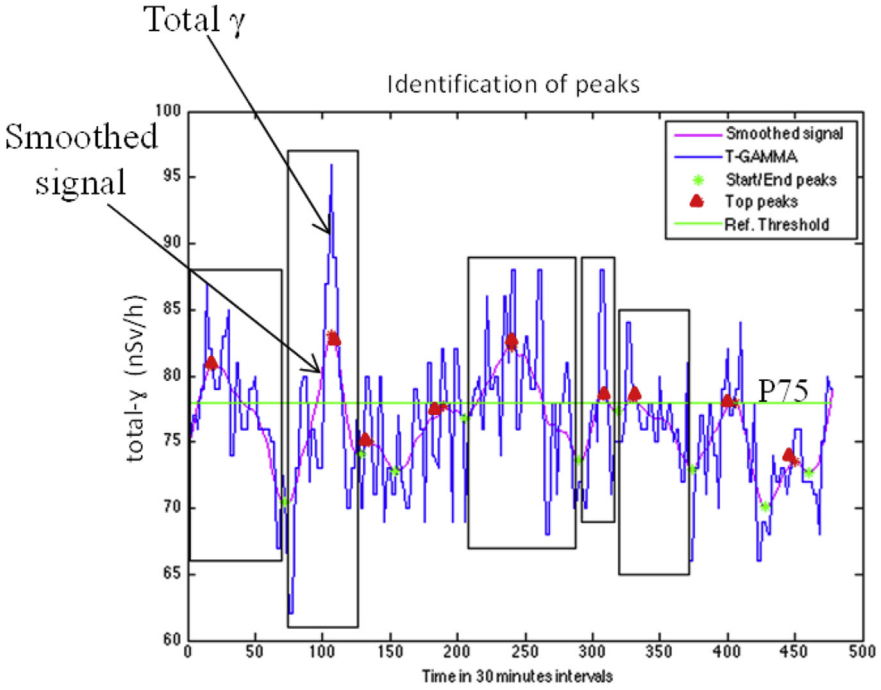

Fig. 7. Example of applying the methodology to the total-γ time (gross ambient dose rate) series and periods selected.

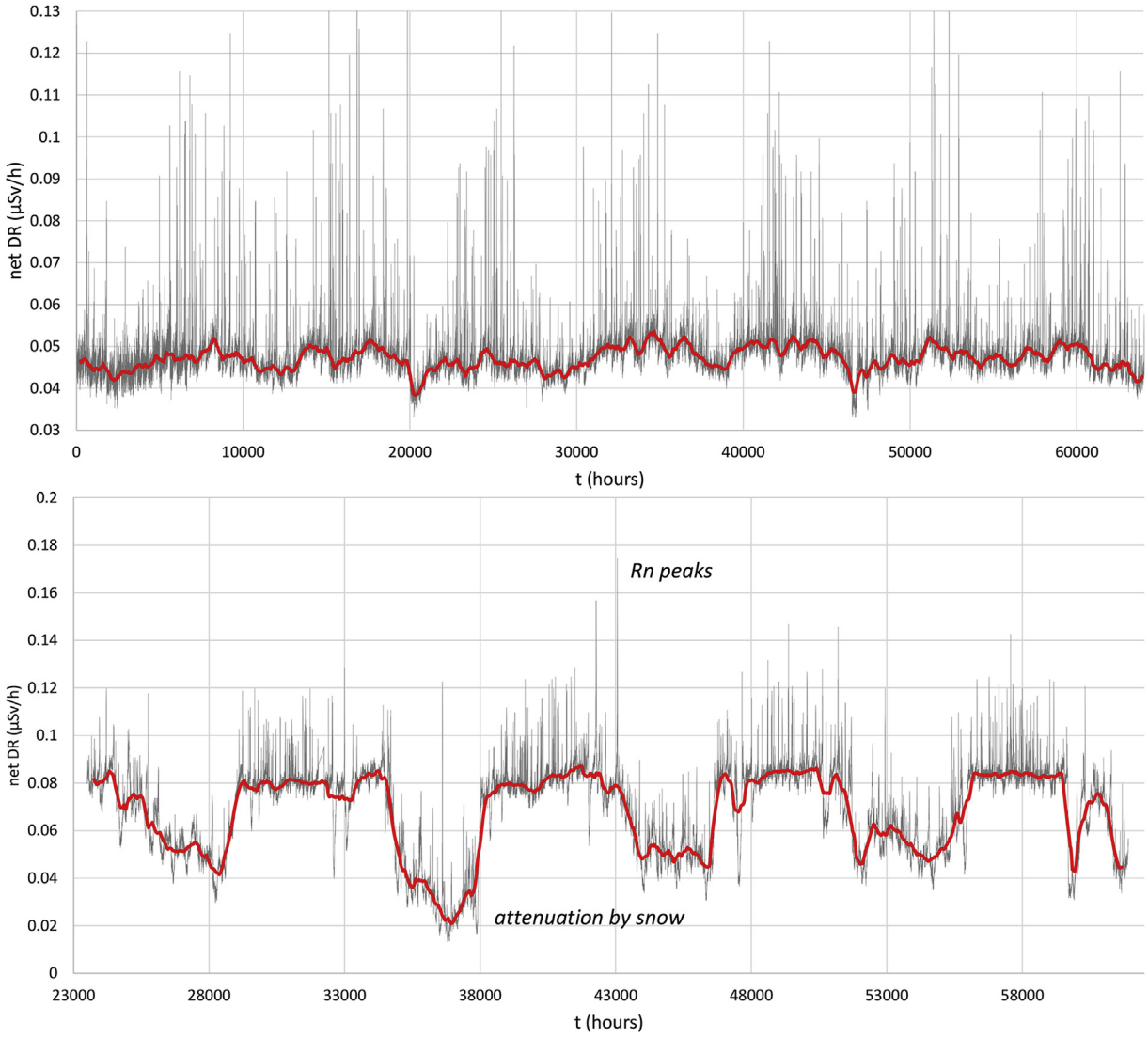

Fig. 8. Two examples of ambient dose rate series. Self-effect and cosmic component subtracted. Grey: net signal, red: estimated terrestrial background. Upper graph: a lowland station, little snow effect; lower graph: a high mountain station, strongly affected by attenuation by long lasting snow cover. (For interpretation of the references to colour in this figure legend, the reader is referred to the web version of this article.)

In both cases self-effect and SCR contribution have been subtracted. The Rn peaks can be recognized clearly; they can amount to a multiple of the terrestrial background. Periodicity is apparent, related to meteorological seasonality. The upper graph comes from a lowland station[8] with little snow effect, but episodes of enhanced terrestrial BG, probably related to dry soil (total 7.3 years). The lower graph shows the series from a station in the mountains[9] with snow cover for several months every year (total 4.4 years). At one instance, the terrestrial dose rate has been reduced to one quarter of the no-snow level, around 0.08 µSv/h.

4.2. Comparison of methods

Methods 1 and 2 are compared in Fig. 9 and Fig. 10. The former shows how the estimated values of the terrestrial BG follow the raw values; in the latter, the results for the methods per time window are shown as scatter plot. Deviations in individual windows are mostly less than 2 nSv/h, i.e. irrelevant for our purposes. The final means, characterizing the terrestrial background at the location, differ for less than 0.04 nSv/h in this example.

The results of methods 2 and 3 applied to all Belgian stations are shown as scatter plot in Fig. 11. In these plots each data point represents the overall mean per station, differently from the above comparison, where estimates per windows, pertaining to one time series, were compared. The results of method 2 include snow periods. Excluding them decreases the squared Pearson correlation from 0.994 to 0.990, since method 3 does so far not include that option. Again, the methods are consistent, in our opinion.

4.3. Uncertainties

Although the methods for separating the terrestrial component work differently, their results are consistent, and thus no important uncertainty seems to result from them. This is quite different for the input parameters, notably self-effect (section 2.2.1), cosmic

[8] Station AT-2008, Vienna Breitenlee (Austria), 163 m asl., 28 Sept 2007–23 Jan 2015.

[9] Station AT-2102, Patscherkofel, Tyrol (Austria), 2240 m asl., 6 Sept 2010–23 Jan 2015.

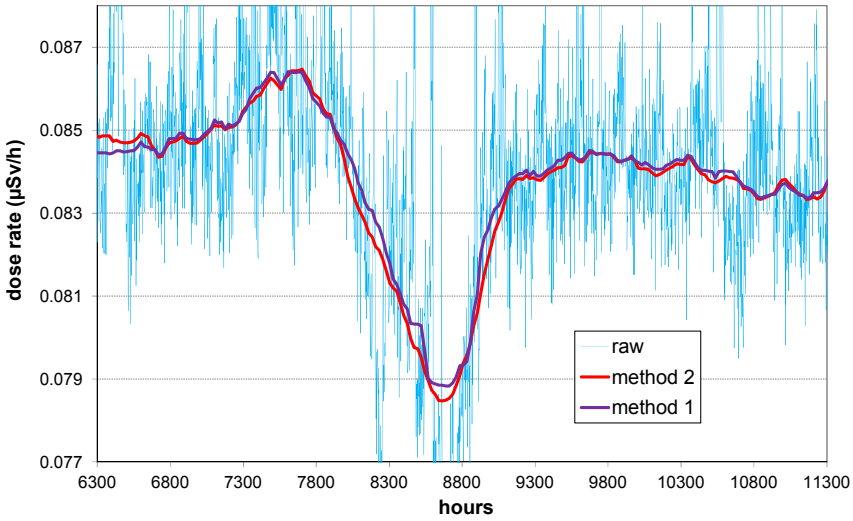

Fig. 9. Performances of methods 1 and 2, small section of a dose rate series.

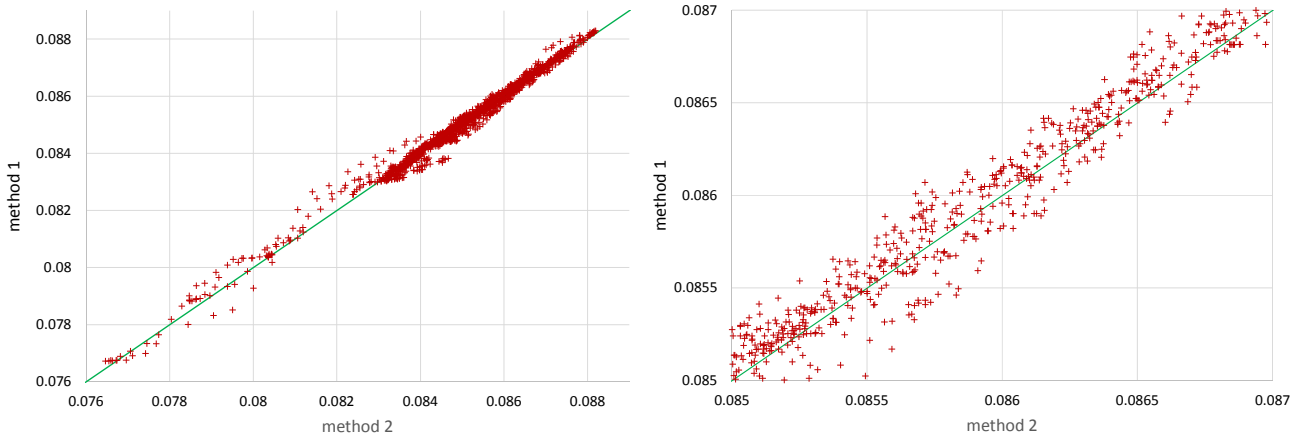

Fig. 10. Comparison of methods 1 and 2, one dose rate series. Right: magnification of a small section of the left graph. Green lines: hypothetical method 1 = method 2. (For interpretation of the references to colour in this figure legend, the reader is referred to the web version of this article.)

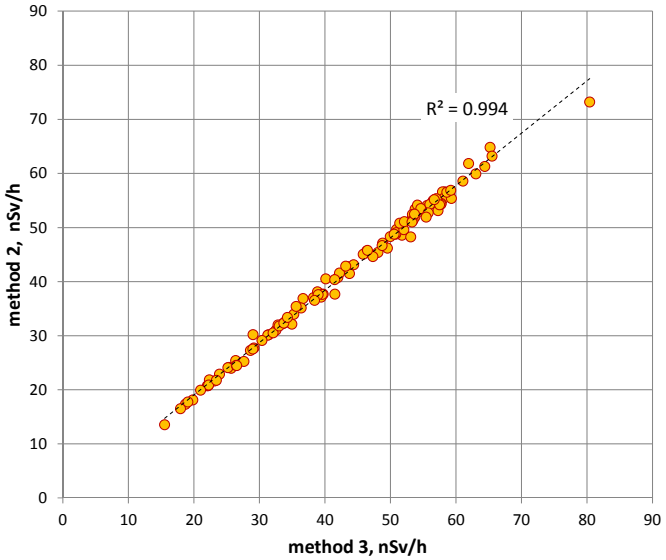

Fig. 11. Comparison of methods 2 and 3, for Belgian stations.

response (section 2.2.2) and site characteristic (section 2.5), which are known differently well for different networks (Table 3 for Austria, Belgium and Germany).

Uncertainty of the self-effect is low, perhaps 1–2 nSv/h, stemming from the variance in a detector population (but not applicable for the German detectors, where each one has been characterized individually). Uncertainty in estimating the SCR components stems from true variability with latitude and solar cycle (on short-term also from weather episodes) and from imperfect knowledge of detector response to SCR. For G-M counters a combined uncertainty of roughly 15% appears reasonable.

Uncertainty, which originates from detector calibration and response to the spectrum of terrestrial radiation (which also varies locally with geochemical composition), has not yet been investigated in detail, to our knowledge. The uncertainty stemming from imperfect site geometry can be considerable (Zähringer and Sempau, 1996, 1997 and follow-up studies), but can be reduced by selecting stations which meet certain site criteria more accurately.

Not considering minor contributions of Rn progenies and anthropogenic fallout, introduces a bias or systematic error in that the terrestrial BG is overestimated. The bias is location dependent,

Table 3
Availability of parameters and data necessary to estimate the terrestrial dose rate component, for Austria, Belgium and Germany.

Effect	Availability of data
Self-effect	Well known only for German probes; for Austria and Belgium: estimated population means
Cosmic response	Relatively well explored for German probes, but some minor issues remaining. Austria, Belgium: generic models.
Site characteristic	Available for many Austrian, all Belgian and German sites
Fallout	Data available for German sites, to be evaluated; Austria: relatively detailed fallout map available.
Rn contribution	Relevance to be explored. Outdoor Rn data available for Germany.

since these components show a geographical trend. The contribution of Rn progenies should be below 5 nSv/h in most of Europe. Fallout should contribute less than 5 nSv/h in most of Europe, but up to 30 or more locally, and several 100 nSv/h in parts of Ukraine, Belarus and Russia.

Random uncertainty consists in the variability mainly of meteorological conditions over the years, which enter the estimates of the terrestrial background via mean soil humidity and snow cover. Variability of the latter is a factor in particular in upland areas. It would be interesting to assess whether climatic change could be visible in dose rate series.

Finally, another component of uncertainty consists in the response of detectors to environmental conditions. Temperature drift can induce a bias over short periods, but also long-term drift effects exist.

5. Conclusions

We gave an overview on the physical effects, which contribute to ambient dose equivalent rate, as registered by monitors of European early warning systems that contribute to EURDEP. (The findings also apply to other dose rate monitors.) We showed how the terrestrial component, i.e. from gamma emitting radionuclides in the ground, could be separated. We also discussed uncertainties induced by model inaccuracy (missing or ill-defined components) and parameter uncertainty, only qualitatively at this stage, however. We further showed algorithms, which are able to separate the terrestrial component automatically, and gave examples of their performances. So far, the analyses were performed for Austrian, Belgian and German monitoring stations.

The main obstacle, at present, for analysing stations of other networks, is lack of some necessary parameters. The gross dose rate data themselves are available from the EURDEP repository, in principle. For most networks, some of the necessary parameters are available from AIRDOS, at least as generic estimates, but not sufficient for performing the analyses shown here. For Austria, Belgium and Germany, availability of data is summarized in Table 3. As a final remark, only to stress it again, one indispensable prerequisite for the success of establishing a European database of terrestrial background radiation is methodical harmonisation.

The methods have been applied to Austrian, Belgian and German stations, so far. First, preliminary evaluations have been shown in Bossew (2015) and Bossew et al. (2015a,b,c). However, this, as well as relation to geology, radionuclide concentrations in top soil etc., is not subject of this article. A future article will be devoted to these topics.

Further work shall include the following topics:

- Data: To extend the analysis to other networks, we shall need better information on parameters for self-effect and cosmic response, as well as about detector set-up and site geometry; the latter for being able to decide whether the data from a certain station can be used at all for estimating the terrestrial component. We hope that the ongoing EU project “Metro ERM”, http://earlywarning-emrp.eu/, will improve the databases.
- Validation of time series: We shall have to develop an automatic algorithm, which is able to identify breakpoints in series, i.e. “steps” due to change of probes or modification of site geometry.
- Refined time series analysis: Fourier, wavelet and Hurst analysis could lead to better understanding the residual variability. If simultaneous meteorological records are available for a monitoring site, correlation between dose rate and these environmental variables could be investigated. (We thank the reviewers for suggestions.)
- Contribution of fallout: For the sake of accuracy one should attempt subtracting the anthropogenic component. How this can be resolved in practice is an open problem at present.
- “Minor contributions”: outdoor Rn can contribute non-negligibly at some locations. The question shall be examined further.
- Cosmic radiation - minor effects: we want to mention the slight latitude dependence and seasonal and solar cycle related periodicity, which one may include in the model. However this makes sense only if the response of probes to SCR is well known at all.
- Snow and other mid-term effects: The “slow” fluctuations due to snow cover, soil humidity and possibly frozen soil are a challenge to automatic analysis. The impact of accounting for such effects on the result (a reasonably precise and accurate[10] value of the mean terrestrial BG at a location) is probably small, in most cases, however.

References

AIRDOS (n.y.): Bossew P., De Cort M., Dubois G., Stöhlker U., Tollefsen T., Wätjen U.: Evaluation of Existing Standards of Measurement of Ambient Dose Rate; and of Sampling, Sample Preparation and Measurement for Estimating Radioactivity Levels in Air. AA N° TREN/NUCL/S12.378241 JRC Ref. N° 21894-2004-04 A1CO ISP BE. Download from the private section of EURDEP, https://eurdep.jrc.ec.europa.eu/Basic/Pages/Private/Downloads/Default.aspx (accessed 20.10.15).

Beck, H.L., DeCampo, J., Gogolak, C., 1972. In Situ Ge(Li) and Nal(Tl) Gamma-ray Spec-trometry. Report HASL-258.

Bleher, M., Doll, H., Stöhlker, U., 2014. Long-term inter-comparison experiment for dose rate and spectrometric probes. Radiat. Prot. Dosim. 160 (4), 306–310.

Bossew, P., Ditto, M., Falkner, Th, Henrich, E., Kienzl, K., Rappelsberger, U., 2001. Contamination of austrian soil with Cs-137. J. Environ. Radioact. 55, 187–194.

Bossew, P., 2015. Estimation of Radon Prone Areas from the Geogenic Radon Potential or Proxy Quantities, Calibrated by Indoor Radon Concentration. Presentation, IAMG 2015, Freiberg, Germany, 6–10 September 2015.

Bossew, P., Cinelli, G., Cernohlawek, N., Gruber, V., Friedmann, H., Dehandschutter, B., Menneson, F., Garcia-Talavera, M., Da Silva, N., Tollefsen, T., Nishev, A., Hernandez-Ceballos, M.A., de Cort, M., 2015a. Can Ambient Dose Rate Be Used for Predicting the Geogenic Rn Potential? Presentation, Conference Radon in the Environment, Krakow (Poland), 26 – 29 May 2015. http://radon.ifj.edu.pl/eng/htdocs/main.php?c=radon_2015 (accessed 21.10.15).

Bossew, P., Cinelli C, G., Cernohlawek, N., Gruber, V., Menneson, V., Tollefsen, T., Nishev, A., Hernández-Ceballos, M.A., de Cort, M., 2015b. Can Terrestrial Gamma Dose Rate Serve as Predictor of Geogenic Radon. Presentation, Conference Rad-2015, Budva (Montenegro), 8–12 June 2015. http://www.rad2015.rad-conference.org/news.php (section radon-thoron) (accessed 05.02.16).

Bossew, P., Cinelli, G., Tollefsen, T., Gruber, V., De Cort, M., 2015c. Estimation of the Geogenic Radon Potential and Radon Prone Areas from Geochemical Quantities and Ambient Dose Rate. Presentation, ENVIRA 2015, Thessaloniki, Greece,

[10] *accurate* – low bias or systematic error; *precise* – low dispersion or random uncertainty.

21–25 September 2015.
Bouville, A., Lowder, W.M., 1988. Human population exposure to cosmic radiation. Radiat. Prot. Dosim. 24 (1–4), 293–299.
Cinelli, G., Hernández-Ceballos, M.A., Bossew, P., Tollefsen, T., Sanchez, I., Marín-Ferrer, M., Nishev, A., Bogučarskis, K., Gruber, V., De Cort, M., 2014. A Method to Estimate the Terrestrial Component of Ambient Dose Equivalent Rate from EURDEP Routine Monitoring Data to Improve the European Geogenic Radon Map. 12th International workshop on the Geological Aspects of Radon risk Mapping, Czech Geological Survey and Radon vos, Prague. ISBN 978-80-01-05548-9, 45-50. JRC91086.
Cinelli, G., Tollefsen, T., Bossew, P., Gruber, V., De Cort, M., 2015. The European Atlas of Natural Radiation. Presentation, Conference Rad-2015, Budva (Montenegro), 8–12 June 2015. http://www.rad2015.rad-conference.org/news.php (section radon-thoron) (accessed 05.02.16).
Clouvas, A., Xanthos, S., Antonopoulos-Domis, M., Silva, J., 2000. Monte Carlo calculation of dose rate conversion factors for external exposure to photon emitters in soil. Health Phys. 78 (3), 295–302.
De Cort, M., et al., 1998. Atlas of the Caesium Deposition on Europe after the Chernobyl Accident. Report EUR 16733. https://rem.jrc.ec.europa.eu/remweb/pastprojects/atlas.aspx (accessed 24.10.15).
De Cort, M., Gruber, V., Tollefsen, T., Bossew, P., Janssens, A., 2011. Towards a European atlas of natural radiation: Goal, status and future perspectives. Radioprotection 46 (6), s737–s743.
Dombrowski, H., Neumaier, S., Thompson, I.M.G., Wissmann, F., 2009. EURADOS intercomparison 2006 to harmonise European early warning dosimetry systems. Radiat. Prot. Dosim. 135 (1), 1–20.
Gasser, E., Nachab, A., Nourreddine, A., Roy, Ch, Sellam, A., 2014. Update of ^{40}K and ^{226}Ra and ^{232}Th series γ-to-dose conversion factors for soil. J. Environ. Radioact. 138, 68–71.
ICRU-51: Intl, September 1993. Commission on radiation Units and measurements: quantities and units in radiation protection dosimetry. Report 51 (1).
ICRU-53: Intl, December 1994. Commission on radiation Units and measurements: gamma-ray spectrometry in the environment. Report 53 (1).
Kümmel, M., Dushe, C., Müller, S., Gehrcke, K., 2014. Outdoor ^{222}Rn-concentrations in Germany – part 1 – natural background. J. Environ. Radioact. 132, 123–130.
Lebedyte, M., Butkus, D., Morkūnas, G., 2003. Variations of the ambient dose equivalent rate in the ground level air. J. Environ. Radioact. 64 (2003), 45–57.
Lee, C.C., Ballinger, T.J., Domino, N.A., 2012. Utilizing map pattern classification and surface weather typing to relate climate to the Air Quality Index in Cleveland, Ohio. Atmos. Environ. 63, 50–59.
Lemercier, M., Gurriaran, R., Bouisset, P., Cagnat, X., 2008. Specific activity to H*(10) conversion coefficients for in situ gamma spectrometry. Radiat. Prot. Dosim. 128 (1), 83–89.
Lowder, W.M., O'Brien, K., 1972. Cosmic-ray Dose Rates in the Atmosphere: Report HASL-254 (New York).
Luff, R., Zähringer, M., Harms, W., Bleher, M., Prommer, B., Stöhlker, U., 2014. Open-source hardware and software and web application for gamma dose rate network operation. Radiat. Prot. Dosim. 160 (4), 252–258.
Malins, A., Okumura, M., Machida, M., Takemiya, H., Saito, K., 2015a. Fields of View for Environmental Radioactivity arXiv:1509.09125v1.
Malins, A., Machida, M., Saito, K., 2015b. Comment on 'Update of ^{40}K and ^{226}Ra and ^{232}Th series γ-to-dose conversion factors for soil. J. Environ. Radioact. 144, 181, 179–180; Reply by Nachab A., ibid.
Menneson, F., Sonck, M., Brouckaert, J.F., n De Gaucquier, M., Léonet, F., 2015. Belgian results from the 3rd EURADOS Intercomparison Study of Environmental monitoring stations. International Symposium of the Belgian Association of Radiological Protection BVS-ABR. April 2015.
Mercier, J.-F., Tracy, B.L., d'Amours, R., Chagnon, F., Hoffman, I., Korpach, E.P., Johnson, S., Ungar, R.K., 2009. Increased environmental gamma-ray dose rate during precipitation: a strong correlation with contributing air mass. J. Environ. Radioact. 100 (7), 527–533.
Murith, C., Gurtner, A., 1994. Mesures in situ et irradiation externe. In: Umweltradioaktivität und Strahlendosen in der Schweiz, Jahresbericht 1993, Bundesamt für Gesundheit. Abteilung Strahlenschutz, Bern, Switzerland' page B-3.3.3 (in French). http://www.iaea.org/inis/collection/NCLCollectionStore/_Public/26/029/26029351.pdf (accessed 04.02.16).
Neumaier, S., Dombrowski, H., 2014. EURADOS intercomparisons and the harmonisation of environmental radiation monitoring. Radiat. Prot. Dosim. 160 (4), 297–305.
Quindos, L.S., Fernández, P.L., Ródenas, C., Gómez-Arozamena, J., Arteche, J., 2004. Conversion factors for external gamma dose derived from natural radionuclides in soil. J. Environ. Radioact. 71, 139–145.
Rybach, L., Medici, F., Schwarz, G.F., 1997. Construction of Radioelement and Dose-rate Baseline Maps by Combining Ground and Airborne Radiometric Data; in: Uranium Exploration Data and Techniques Applied to the Preparation of Radioelement Maps, IAEA-tecdoc-980. IAEA, Vienna, pp. 33–44. http://www.iaea.org/inis/collection/NCLCollectionStore/_Public/29/009/29009822.pdf (accessed 20.10.15).
Sáez-Vergara, J.C., Thompson, I.M.G., Gurriarán, R., Dombrowski, H., Funck, E., Neumaier, S., 2007. The second EURADOS intercomparison of national network systems used to provide early warning of a nuclear accident. Radiat. Prot. Dosim. 123 (2), 190–208.
Saito, K., Jacob, P., 1995. Gamma ray fields in the air due to sources in the ground. Radiat. Prot. Dosim. 58 (1), 29–45.
Saito, K., Petoussi-Henss, N., 2014. Ambient dose equivalent conversion coefficients for radionuclides exponentially distributed in the ground. J. Nucl. Sci. Technol. 51 (10), 1274–1287.
Smetsers, R.C.G.M., Blaauboer, R.O., 1994. Time-resolved monitoring of outdoor radiation levels in the Netherlands. Rad. Prot. Dosim. 55 (3), 173–181.
Smetsers, R.C.G.M., Blaauboer, R.O., 1997a. A dynamic compensation method for natural ambient dose rate based on 6 years data from the Dutch radioactivity monitoring network. Rad. Prot. Dosim. 69 (1), 19–31.
Smetsers, R.C.G.M., Blaauboer, R.O., 1997b. Source – dependent probability densities explaining frequency distributions of ambient dose rate in the Netherlands. Rad. Prot. Dosim. 69 (1), 33–42.
Spiers, F.W., Gibson, J.A.B., Thompson, I.M.G., 1981. A Guide to the Measurement of Environmental Gamma-ray Dose Rate. National Physical Laboratory, Teddington, Middlesex, UK. report on behalf of British Committee on Radiation Units and Measurements. ISBN 0-9504496-7-9;available at: http://cds.cern.ch/record/1057200/files/CM-P00066948.pdf (accessed 27.10.15).
Stöhlker, U., Bleher, M., 2007. INTAMAP Deliverable 5–1: Identifying Anomalies with Monitoring Networks and 5-2: from National to International Networks. http://www.intamap.org/publications.php#deliverables (accessed 23.10.15).
Stöhlker, U., Bleher, M., Conen, F., Bänninger, D., 2012. Harmonization of ambient dose rate monitoring provides for large scale estimates of radon flux density and soil moisture changes. In: Sources and Measurements of Radon and Radon Progeny Applied to Climate and Air Quality Studies Proceedings of a Technical Meeting Held in Vienna, Organized by the International Atomic Energy Agency and Co-sponsored by the World Meteorological Organization. IAEA Proceedings series. http://www-pub.iaea.org/MTCD/publications/PDF/P1541_web.pdf (accessed 24.10.15).
Szegvary, T., Conen, F., Stöhlker, U., Dubois, G., Bossew, P., de Vries, G., 2007a. Mapping terrestrial γ-dose rate in Europe based on routine monitoring data. Radiat. Meas. 42, 1561–1572.
Szegvary, T., Leuenberger, M.C., Conen, F., 2007b. Predicting terrestrial 222Rn flux using gamma dose rate as a proxy. Atmos. Chem. Phys. 7, 2789–2795. www.atmos-chem-phys.net/7/2789/2007/ (accessed 24.10.15).
Tandon, A., Attri, A.K., 2011. Trends in total ozone column over India: 1979–2008. Atmos. Environ. 45, 1648–1654.
Wissmann, F., Dangendorf, V., Schrewe, U., 2005. Radiation exposure at ground level by secondary cosmic radiation. Radiat. Meas. 39, 95–104.
Wissmann, F., 2006. Variations observed in environmental radiation at ground level. Radiat. Prot. Dosim. 118 (1), 3–10.
Wissmann, F., Sáez-Vergara, J.C., 2006. Dosimetry of environmental radiation – a report on the achievements of EURADOS WG3. Radiat. Prot. Dosim. 118 (2), 167–175.
Wissmann, F., Rupp, A., Stöhlker, U., 2007. Characterization of dose rate instruments for environmental radiation monitoring. Kerntechnik 72, 193–198.
Zähringer, M., Sempau, J., 1996. The assessment of the representativeness of data from dose rate monitoring stations. Radiat. Prot. Dosim. 64 (4), 275–282.
Zähringer, M., Sempau, J., 1997. Calibration Factors for Dose Rate Probes in Environmental Monitoring Networks Obtained from Monte Carlo Simulations. BfS report BfS-IAR-2/97.